Published in final edited form as:
Mol Pharm. 2010 August 2; 7(4): 936–943. doi:10.1021/mp100054m.

An Effective Targeted Nanoglobular Manganese(II) Chelate Conjugate for Magnetic Resonance Molecular Imaging of Tumor Extracellular Matrix

Mingqian Tan[1], **Xueming Wu**[1], **Eun-Kee Jeong**[2], **Qianjin Chen**[3], **Dennis L. Parker**[2], and **Zheng-Rong Lu**[1,*]

[1]Department of Biomedical Engineering, Case Western Reserve University, Cleveland, OH 44106

[2]Department of Radiology, University of Utah, Salt Lake City, UT 84108

[3]Department of Chemistry, The Chinese University of Hong Kong, Hong Kong

Abstract

Stable manganese(II) chelates are of great interest for the design and development of safe and effective non-gadolinium(III)-based targeted MRI contrast agents for MR cancer molecular imaging. In this study, a CLT1 peptide targeted G3 nanoglobular Mn(II)-DOTA monoamide conjugate was designed and synthesized as a targeted MRI contrast agent for molecular imaging of the fibrin-fibronectin complexes or oncofetal fibronectin in tumor stroma. The targeted contrast agent comprised of 2 peptides and 42 Mn(II)-DOTA chelates on the surface of the G3 nanoglobule. The T_1 and T_2 relaxivities of the targeted agent at room temperature were 3.13 and 8.14 $mM^{-1}sec^{-1}$ per Mn(II) chelate at 3T, respectively. It had a well-defined nanosize (5.2 nm) and could be readily excreted via renal filtration. The targeted nanoglobular contrast agent specifically bound to tumor tissue, resulting in significant tumor contrast enhancement with minimal non-specific enhancement in the liver in tumor-bearing mice as compared to a non-targeted control at a dose as low as 0.03 mmol-Mn/kg. The targeted G3 nanoglobular Mn(II)-DOTA conjugate is promising as a targeted non-gadolinium(III) based MRI contrast agent for MR cancer molecular imaging.

Keywords

MR molecular imaging; Manganese(II); targeted contrast agent; peptide; nanoglobule

1. Introduction

Molecular imaging enables the direct visualization of disease related biomarkers for earlier and accurate detection and diagnosis of life-threatening diseases. Currently, optical imaging and nuclear medicine are the commonly used imaging modalities for molecular imaging due to their high sensitivity. However, optical imaging is limited by low tissue penetration and nuclear medicine is limited by low spatial resolution. Magnetic resonance imaging (MRI) is a powerful clinical imaging modality for soft tissue imaging without ionizing radiation. Contrast enhanced MRI can be used for molecular imaging if a target-specific contrast agent can generate detectable contrast enhancement at the target of interest. Due to the low sensitivity of MRI, various nanosized targeted contrast agents, including Gd(III) containing

*Correspondence to: Dr. Zheng-Rong Lu, Department of Biomedical Engineering, Wickenden Building, Room 427, Case Western Reserve University, 10900 Euclid Avenue, Cleveland, OH 44106-7207, zxl125@case.edu.

micelles and liposomes, and superparamagnetic iron oxide nanoparticles (SPIO) have been designed to produce sufficient contrast enhancement for effective MRI molecular imaging.[1-5] Unfortunately, these nanosized agents are too big to be excreted through renal filtration after imaging. Slow excretion of Gd(III) based contrast agents may cause serious toxic side effects.[6] There is a need to develop new effective non-gadolinium(III) based targeted nanosized MRI contrast agents to alleviate the safety concern related to Gd(III)-based nano-sized targeted contrast agents for MR molecular imaging.

Manganese(II) ion has relatively high electronic spins (5/2) and fast water exchange rates and its chelates can be used to develop targeted MRI contrast agents.[7, 8] Mn(II) ion is an essential component of cells and a cofactor for enzymes and receptors and the side effects of Mn(II) based agents could be lower than Gd(III) based agents.[9] Mn(II)-based MRI contrast agents have been investigated over the past decades. A hepatocyte-specific agent Mn(II) dipyridoxal diphosphate (Mn-DPDP) and an oral agent containing $MnCl_2$ (LumenHance) have been developed for clinically applications.[10] However, Mn(II) based contrast agents remain relatively less studied because of their low relaxivity as compared to Gd(III)-based MRI contrast agents. This limitation can be overcome by incorporating multiple Mn(II) chelates in a nanosized contrast agent to increase the overall relaxivities of the agent. The incorporation of a targeting agent into the Mn(II)-based nanosized contrast agent may result in a safe and effective targeted nanosized Mn(II) based contrast agent for MR molecular imaging.

Dendrimers are a unique class of polymers with well-defined structure and nanosize.[11] The large number of functional groups on their surface serves as a platform for conjugating contrast agents and targeting moieties to in the design of targeted MRI contrast agents with improved sensitivity and specificity.[12] We have recently designed and developed poly-$_L$-lysine dendrimers with an octa(3-aminopropyl)silsesquioxane (OAS) cubic core, the nanoglobules, as novel well defined carriers for MRI contrast agents.[13, 14] These macromolecules have well-defined nanosizes (3.7 nm for the generation 3 nanoglobule) and exhibit a relatively compact and rigid three-dimensional structure due to the three-dimensional cubic structure of the core. Gd(III) based contrast agents prepared from the nanoglobules resulted in strong contrast enhancement in the blood pool and tumor tissue and could be readily excreted via renal filtration.[14] Targeted Gd(III) based contrast agents developed from the nanoglobules also resulted in strong target specific contrast enhancement in tumor tissues at a relatively low dose.[15] We hypothesized that the incorporation of a relatively large number of stable Mn(II) chelates into the nanoglobules could result in effective non-Gd(III) based MRI contrast agents with improved relaxivities.

We have recently shown that conjugating CLT1 peptide (CGLIIQKNEC) to Gd(III) chelates result in targeted contrast agents for targeted tumor MR imaging.[15, 16] CLT1 peptide binds to fibrin-fibrinectin complexes or oncofetal fibronectin in the stroma of solid tumors.[17] Since cancer-related fibronectin or fibrin-fibronectin complexes are abundantly present in tumor stroma,[18, 19] a sufficient amount of the targeted contrast agents bind to the tumor tissue, resulting in strong tumor enhancement for MR cancer molecular imaging.[15,16] In this study, we synthesized and investigated a CLT1 targeted G3 nanoglobular Mn(II)-DOTA monoamide conjugate as a targeted non-Gd(III) MRI contrast agent. The targeted nanoglobular agent was characterized by inductively coupled plasma-optical emission spectroscopy (ICP-OES), laser light scattering and MRI. Tumor specific contrast enhancement of CLT1-targeted nanoglobular Mn(II)-DOTA monoamide conjugate was evaluated in mice bearing breast cancer xenografts at a dose as low as 0.03 mmol-Mn/kg.

2. Materials and Methods

Benzotriazol-1-yl-oxytripyrrolidinophosphonium hexafluorophosphate (PyBOP), 2-(1*H*-benzotriazole-1-yl)-1,1,3,3-tetramethyluronium hexafluorophosphate (HBTU), and 1-hydroxybenzotriazole (HOBt) were purchased from Nova Biochem (Darmstadt, Germany). 1,4,7,10-Tetraazacyclododecane-1,4,7-tris-*tert*-butyl acetate-10-acetic acid [DOTA-tris(t-Bu)] was purchased from Macrocyclics (Dallas, TX). Azido-dPEG™$_8$ NHS ester and propargyl-dPEG™$_1$-NHS ester were purchased from Quanta BioDesign (Powell, OH). N,N-Diisopropylethyl amine (DIPEA) and N,N-dimethylformamide anhydrous (DMF) were purchased from Alfa Aesar (Ward Hill, MA). Trifluoroacetic acid (TFA), copper(II) sulfate pentahydrate and ascorbic acid were purchased from ACROS Organics (Morris Plains, NJ). All reagents were used without further purification unless otherwise stated.

Matrix-assisted laser desorption/ionization time of flight (MALDI-TOF) mass spectra were acquired on a Voyager DE-STR spectrometer (PerSpeptive BioSystems) in linear mode with α-cyano-4-hydroxycinnamic acid as a matrix. The Mn(II) content was measured by inductively coupled plasma-optical emission spectroscopy (ICP-OES Optima 3100XL, Perkin Elmer, Norwalk, CT). Amino acid analysis was performed using the Hitachi L-8800 Amino Acid Analyzer (Tokyo, Japan). The sizes of nanoglobular contrast agents were measured by a modified commercial laser light scattering spectrometer (ALV/DLS/SLS-5022F) which is equipped with a multi-τ digital time correlator (ALV5000) and a cylindrical 22 mW He-Ne laser (λ=632.8 nm, Uniphase) as the light source. Nanoglobular agents were purified using 0.1 μm Millipore filters before the measurement.

2.1. Synthesis of G3 nanoglobule-(Mn-DOTA-monoaimde)$_{44}$-(PEG-azido)$_4$ conjugate (compound 1)

Generation 3 (G3) nanoglobule with an OAS core, was synthesized using standard liquid-phase peptide synthesis chemistry (MALDI-TOF (m/z, $[M+H]^+$): 8,054.59 (calculated), 8,054.68 (measured), Fig. S1).13 G3 nanoglobule, (*L*-lysine)$_{32}$-(*L*-Lysine)$_{16}$-(*L*-Lysine)$_8$-octa(3-aminopropyl) silsesquioxane (OAS) trifluoroacetate (107 mg, 6.97 μmol), azido-dPEG™$_8$ NHS ester (23.6 mg, 41.82 μmol), HBTU (16 mg, 41.82 μmol), HOBt (5.6 mg, 41.82 μmol) and DIPEA were dissolved in 3 mL of DMF and magnetically stirred at room temperature overnight. The reaction mixture was added to anhydrous diethyl ether. The resulting precipitate was dissolved in pure water and further purified by ultrafiltration using Millipore's Amicon® Ultra-15 centrifugal filters with molecular weight cutoff of 3 kDa in deionized water. MALDI-TOF (m/z, $[M+H]^+$): 9,857.02 (measured), 9,857.13 (calculated for G3 with 4 azido groups on average) (Fig. S2). The yield of nanoglobule-PEG-azido conjugate was 98 mg, 82.4%.

Nanoglobule-PEG-azido (98 mg, 5.73 μmol), 1,4,7,10-tetraazacyclododecane-1,4,7-tris-*tert*-butyl acetate-10-acetic acid [DOTA-tris(*t*-Bu), 683 mg, 1.2 mmol], HBTU (450 mg, 1.2 mmol), HOBt (160 mg, 1.2 mmol) and excess DIPEA were dissolved in DMF and stirred at room temperature for 24 h. The product was precipitated out by adding anhydrous diethyl ether. The oily precipitate was washed with diethyl ether, and the protective *t*-butyl groups were then removed by treating the precipitate with trifluoroacetic acid and dichloromethane (10 mL, volume/volume = 1:1) for 24 h while stirring at room temperature. The residue was treated with ice-cold diethyl ether to yield a colorless solid precipitate. The precipitate was dissolved in deionized water and further purified by ultrafiltration. MALDI-TOF (m/z, $[M+H]^+$): 26,879 (measured), 26,828 [calculated for G3-(PEG-azido)$_4$ with 44 DOTA on average] (Fig. S3). The yield of G3 nanoglobule-DOTA$_{44}$-(PEG-azido)$_4$ conjugate was 185 mg, 95.5%.

G3 nanoglobule-DOTA$_{44}$-(PEG-azido)$_4$ (50 mg, 1.48 μmol) and manganese(II) acetate salt (117 mg, 480 μmol) in 5 ml ammonium acetate solution were refluxed for 50 min,20 and then the reaction solution was cooled down and the product was purified by ultrafiltration. The product nanoglobule-(Mn-DOTA)$_{44}$-(azido-PEG)$_4$ was further purified by dialysis with a membrane of 1000 Da molecule weight cutoff at room temperature for 96 h. The yield of nanoglobule-(Mn-DOTA)$_{44}$-(PEG-azido)$_4$ was 42 mg, 96.8%.

2.2. Synthesis of peptide-PEG-propargyl conjugate (compound 2)

Standard solid-phase peptide synthesis was employed to synthesize peptide CLT1 (CGLIIQKNEC) from Fmoc-protected amino acids on a 2-chlorotrityl chloride resin. At the end of the peptide synthesis, a short linker, Fmoc-12-amino-4,7,10-trioxadodecanoic acid (532 mg, 1.2 mmol) in DMF was reacted with the peptide (960 mg, 0.4 mmol) on the beads under the presence of HOBt (162 mg, 1.2 mmol), PyBop (624 mg, 1.2 mmol) and excess DIPEA at room temperature for 1 h. After removing the Fmoc group with piperidine DMF solution, propargyl-dPEG™$_1$-NHS ester (270 mg, 1.2 mmol), HOBt (162 mg, 1.2 mmol), PyBop (624 mg, 1.2 mmol) and DIPEA in DMF were added and reacted at room temperature for 1 h to conjugate propargyl group at the N-terminal of the peptide. The peptide-PEG-propargyl conjugate was then cleaved from the resin using trifluoroacetic acid solution containing 2.5% 1,2-ethanedithiol, 2.5% water, and 1.0% triisobutylsilane. The product was exposed to air to allow the formation of disulfide bonds for the cyclic peptide. MALDI-TOF (m/z, $[M+H]^+$): 1,431.68 (calculated), 1,431.68 (observed) (Fig. S4). The yield of peptide-PEG-propargyl conjugate was 320 mg, 55.9%.

2.3. Preparation of CLT1 peptide targeted nanoglobular Mn(II) chelate contrast agent (compound 3)

The conjugation of CLT1 peptide to G3 nanoglobule-(Mn-DOTA)$_{44}$-(PEG-azido)$_4$ conjugate was carried out by “click chemistry” 21between the reactive propargyl group of the peptide and azide group of the nanoglobule-(Mn-DOTA)$_{44}$-(PEG-azido)$_4$. Nanoglobule-(Mn-DOTA)$_{44}$-(PEG-azido)$_4$ conjugate (42 mg, 1.43 μmol) and ascorbic acid (5 mg, 28 μmol) was dissolved in 2 mL water and mixed with copper(II) sulfate pentahydrate (1.4 mg, 5.6 μmol) and peptide-PEG-propargyl conjugate (12.3 mg, 8.58 μmol) in 2 mL *tert*-butyl alcohol. The reaction solution was stirred for 24 h at room temperature. After grafting, any precipitate in the reaction solution was removed by filtration. The product was purified first by ultrafiltration (molecule weight cutoff = 3000 Da), and then by dialysis (molecule weight cutoff = 1000 Da) at room temperature to remove any small molecular impurities. The yield of the targeted nanoglobular Mn(II) chelate was 36 mg, 80%. The Mn(II) content was measured by ICP-OES. The average number of peptide conjugated to the nanoglobular surface was determined by amino acid analysis and estimated from sulfur content determined by ICP-OES.

2.4. Synthesis of non-targeted nanoglobular Mn(II) chelate contrast agent

Non-targeted nanoglobular Mn(II) chelate was synthesized as a control following the same procedures used for the preparation of targeted agent. G3 nanoglobule (50 mg, 3.26 μmol), DOTA-tris(*t*-Bu) (238 mg, 416 μmol), HBTU (158 mg, 416 mmol), HOBt (56 mg, 416 mmol) and DIPEA (1.2 mL) were dissolved in DMF and stirred at room temperature for 24 h. The product was precipitated by mixing the reaction solution with anhydrous diethyl ether. The oily precipitate was washed with diethyl ether 3 times. After removing the protective *t*-butyl groups with a mixture of trifluoroacetic acid and dichloromethane (6 mL, volume/volume = 1:1), the residue was treated with ice-cold diethyl ether to give a colorless solid precipitate. The dried precipitate was dissolved in pure water and further purified by ultrafiltration. MALDI-TOF (m/z, $[M+H]^+$): 28,946 (calculated for G3 with 54 DOTA on average), 28,785 (observed, Fig. S6). The yield of G3 nanoglobule-DOTA conjugate was 85

mg, 91%. G3 nanoglobule-$(DOTA)_{54}$ was complexed with Mn(II) following the procedure for targeted agent in section 2.1 to gave G3 nanoglobule-$(Mn\text{-}DOTA)_{54}$ as a colorless solid. The Mn(II) content was measured by ICP-OES.

2.5. Measurement of r_1 and r_2 relaxivities of the nanoglobular contrast agents

The r_1 and r_2 relaxivities of the contrast agents were determined on a Siemens 3T MRI scanner at room temperature in aqueous solutions. Longitudinal relaxivity (r_1) of the contrast agents was determined by measuring the water proton T_1 relaxation times for different concentrations of the agents and for a water reference using an inversion recovery prepared turbo spin echo imaging pulse sequence. The inversion times (TI) were 25, 35, 50, 75, 100, 200, 400, 800, 1600, and 3200 ms with repetition time (TR) = 5000 ms and echo time (TE) = 16.0 ms. The net magnetization from the region of interest of each sample was fit using a Marquardt-Levenberg algorithm for multiparametric nonlinear regression analysis using MATLAB program. T_1 and M_0 were calculated from these data and r_1 was determined from the slope of $1/T_1$ versus $[Mn^{2+}]$ plot. Transverse relaxivity (r_2) was determined by measuring the T_2 relaxation times of the samples using a turbo spin echo sequence with a turbo factor of 3. The parameters were as follows: TE = 12, 24, 35, 47, 59, 71, 83, 94 and 106 ms; TR = 3000 ms. T_2 value for a given concentration was calculated from $M_{TE} = M_0 e^{(-TE/T_2)}$ after non-linear regression with various TE. Transverse relaxivity, r_2, was determined from the slope of $1/T_2$ versus $[Mn^{2+}]$ plot.

2.6. Animal Tumor Model

Female athymic nu/nu mice (4-6 weeks old), weighted 20-25g, were purchased from the National Cancer Institute (Frederick, MD). The mice were subcutaneously implanted in the both flanks with 2×10^6 MDA-MB-231 breast carcinoma cells in a mixture of 50 μL culture medium and 50 μL Matrigel. MDA-MB-231 cell line was purchased from ATCC (Manassas, VA). The MRI study was performed when the tumor size reached 0.5-1.0 cm in diameter 3 weeks later. The mice were randomly divided into groups with three mice for each group for MRI study.

2.7. Contrast Enhanced MRI

The mice were anesthetized with an intraperitoneal injection of a mixture of 12 mg/kg xylazine and 80 mg/kg ketamine. The anesthetized mice were placed on a heating pad all the time before the MRI study and then wrapped in a warm towel to maintain body temperature at 35 °C during MRI scanning. MRI contrast agents were administered at the tail vein at a dose of 0.03 mmol-Mn/kg. The mice were placed in a human wrist coil and scanned in a Siemens Trio 3T MRI scanner at pre-injection and at 2, 5, 10, 15, 20 and 25 min post-injection using a fat suppression 3D FLASH sequence (TR=7.8 ms, TE=2.74 ms, 25° flip angle, 0.4 mm slice thickness). Axial tumor MR images were also acquired using a 2D spin-echo sequence (TR=400 ms, TE=8.9 ms, 90° flip angle, 2.0 mm slice thickness). *In vivo* contrast enhancement of the blood pool was analyzed using Osirix software. Contrast to noise ratios (CNR) were measured at each time point and averaged from three different mice (N=3) for the tumor. The CNR was calculated using the following equation: $\mathrm{CNR}=\frac{S - S_0}{\sigma_n}$; where S (post-injection) and S_0 (thigh muscle) denote the signal within the regions of interest (ROIs) and σ_n is the standard deviation of noise estimated from the background air. Statistical analysis was performed using a two-way ANOVA with Bonferroni's, assuming statistical significance at $p < 0.05$.

2.8. Immunohistochemistry Study

Mice were sacrificed 24 h post-injection. The MDA-MB-231 tumor tissues were removed, fixed with 3% paraformaldehyde and embedded in paraffin. Immunohistochemistry was performed according to suppliers' protocol (Santa Cruz Biotech., rabbit ABC staining system: cat#sc-2018). Briefly, tissue sections (4 μm thickness) were incubated in 3% hydrogen peroxide and 10% methanol for 10 min at room temperature to block endogenous peroxidase activity. The slides were boiled in antigen retrieval solution (1 mmol/L Tris-HCl, 0.1 mmol/L EDTA, pH=8.0) for 15 minutes at high power in a microwave. The sections were then incubated with primary anti-fibronectin antibody at appropriate dilutions overnight. After washing with phosphate-buffered saline solution, the sections were incubated with biotinylated secondary antibody and a horseradish peroxidase-streptavidin complex, for 1 h each. Tissue samples were then colorized with DAB substrate, counterstained, mounted, and visualized with a bright-field microscope.

3. Results and discussion

Synthesis of the targeted contrast agent

The targeted Mn(II)-based nanoglobular MRI contrast agent was synthesized by stepwise conjugation of Mn(II)-DOTA and CLT1 peptide to G3 nanoglobule, Scheme 1. Mn(II)-DOTA was selected to prepare the targeted nanoglobular contrast agent because of its relative large stability constant (log K_{MnL}=20.2) as compared to Mn(II)-DTPA (log K_{MnL}=15.6) and Mn(II)-EDTA (log K_{MnL}=13.9).22 The stability of Mn(II)-DOTA is also higher than Ca(II)-DOTA (log K_{CaL}=17.23) and Mg(II)-DOTA (log K_{MgL}=13.64).23 The macrocyclic chelates also demonstrate higher kinetic stability over the open-chain chelates. High kinetic stability is critical to minimize transmetallation of paramagnetic chelates with the endogenous metal ions, including Ca^{2+}, Mg^{2+}, Cu^{2+} and Zn^{2+}. Macrocyclic Gd chelates, e.g. Gd(DO3A-HP), have shown much higher kinetic stability against transmetallation against endogenous ions, mainly Zn^{2+}, than open-chain Gd(III) chelates.24 It is expected that the macrocyclic Mn(II) chelate possesses high in vivo kinetic stability against transmetallation.

Azido groups were first introduced onto the generation 3 nanoglobule (G3) by reacting with azido-dPEG™$_8$ NHS ester active. The azido-containing nanoglobule was then reacted with DOTA-tris(*t*-Bu) to yield the azido-containing nanoglobular DOTA conjugate after deprotection with trifluoroacetic acid. Approximately 70% of the surface amine groups of the G3 nanoglobule were conjugated with Mn(II)-DOTA monoamide with 100% excess of DOTA-tris(*t*-Bu) in the conjugation reaction. The conjugate was then reacted with $Mn(OAc)_2$ to give nanoglobule-PEG-azido-(Mn-DOTA) conjugate (compound **1**). CLT1 peptide with a propargyl-PEG linker (compound **2**) was synthesized with standard solid phase peptide chemistry. The CLT1 targeted nanoglobular Mn(II)-DOTA conjugate (compound **3**) was finally prepared by "clicking" compounds **1** with **2** in a *tert*-butyl alcohol/water solution at room temperature. Click chemistry is a convenient and highly selective approach in the stepwise synthesis of targeted nanoglobular contrast agents and no protecting groups are required for attaching the peptide sequence onto the nanoglobular surface. A short PEG spacer was used between the peptide and the nanoglobule to reduce the steric hindrance of the latter on specific binding of the targeted agent. A non-targeted G3 nanoglobular agent was similarly prepared as a control agent.

The physicochemical parameters of the contrast agents are listed in Table 1. The manganese content in the targeted agent was 7.2 wt-%, approximately 42 Mn(II) chelates per nanoglobule on average, as determined by ICP-OES. Two CLT1 molecules on average were conjugated onto the nanoglobule as calculated from amino acid analysis and the sulfur

content determined by ICP-OES. The Mn content in the control nanoglobular Mn(II)-DOTA conjugate was 9.4 wt-%, approximately 54 Mn(II) chelates per nanoglobule. The size of G3 nanoglobule and non-targeted conjugate was approximately 3.7 nm and 4.2 nm, respectively, as measured by dynamic light scattering (Figure 1). The size of the targeted agent was 5.2 nm, due to the incorporation of CLT1 peptide moieties. All of the nanoglobules had a narrowly dispersed size distribution. The order of size distribution of nanoglobules is G3 nanoglobule < non-targeted agent < the targeted agent as shown by dynamic light scattering. The slightly increase of size distribution was due to non-uniform conjugation of Gd-DOTA and peptide in the contrast agents. Nevertheless, the size distribution of the targeted nanoglobular contrast agents was still relatively uniform as compared to that of linear polymeric MRI contrast agents. The sizes of the nanoglobular contrast agents were smaller than the renal filtration threshold (ca. 8 nm),25 which could allow ready clearance of the unbound agent via renal filtration. As shown in Figure 1, all of the nanoglobular compounds had a relatively narrow size distribution. The targeted agent with low polydispersity would allow its penetration through leaky tumor blood vessels without the complications of linear polymers due to their broad size distribution. The r_1 and r_2 relaxivities of the targeted nanoglobular agent were 3.13 and 8.74 $mM^{-1}s^{-1}$ per Mn(II) chelate, and 2.84 and 12.61 $mM^{-1}s^{-1}$ for the non-targeted agent at 3T (Table 1› Figure 2). The T_1 relaxivity of both agents was higher than that of Mn(II)-DOTA (2.6 $mM^{-1}s^{-1}$) measured at low magnetic field.26 The overall relaxivities of the targeted nanoglobular contrast agent were r_1 = 131.46 and r_2 = 367.08 $mM^{-1}s^{-1}$ per nanoglobule. The slight increase of the r_1 relaxivity of the targeted agent is possibly due to the increased particle size by conjugation of peptide molecules to the nanoglobules.

In Vivo MR Imaging

The effectiveness of the CLT1-targeted nanoglobular Mn(II)-DOTA conjugate for MR molecular imaging of the cancer-related fibronectin in tumor was evaluated in female nude mice bearing MDA-MB-231 human breast carcinoma xenografts on a Siemens 3T scanner. Figure 3 shows the 3D maximum intensity projection images of mice before and after intravenous injection of CLT1 targeted nanoglobular agent and the control agent at a dose as low as 0.03 mmol-Mn/kg. Little enhancement was observed in the blood pool and liver for both targeted agent and control. Strong enhancement was observed in the urinary bladder 10 minutes post-injection, indicating renal excretion of the targeted nanoglobular agent. Since the size (~5.2 nm) of CTL1-targeted nanoglobular contrast agent was smaller than the renal filtration threshold (ca. 8 nm),25 the unbound targeted agent was able to readily excrete from the blood circulation and normal tissue through renal filtration. The blood pool enhancement of the targeted contrast agent was less significant than the corresponding Gd(III)-based CLT1-targeted G3 nanoglobular contrast agent (r_1 = 8.20 $mM^{-1}s^{-1}$ per Gd at 3T) at the same dose,15 possibly due to the lower relaxivity of the Mn(II)-based agent.

Figure 4 shows the axial T_1-weighted 2D spin-echo images of tumor tissue before and 25 minutes after intravenous injection of the targeted agent and the control agent. The targeted agent resulted in more significant tumor enhancement than the non-targeted control agent. Quantitative analysis revealed that CTL1-targeted nanoglobular contrast agent resulted in 140% more contrast-to-noise ratio (CNR) in the tumor tissue than the non-targeted agent at two minutes post-injection (Figure 5, $p < 0.05$). High CNR was maintained for the targeted agent throughout the experiment period up to 25 minutes. Although the T_1 relaxivity of the Mn(II)-based targeted agent was lower than that of the corresponding Gd(III)-based CLT1-targeted agent,15 the overall T_1 relaxivity of the Mn(II)-based targeted nanoglobular agent was sufficiently high to generate significant tumor enhancement for effective tumor imaging at the low dose, which is much lower than the commonly used dose for Mn(II) MRI (0.4 mmol-Mn/kg).7

The presence of the fibronectin in the MDA-MB-231 tumor tissue was verified by immunohistochemistry study after *in vivo* MR imaging.15 The CLT1 peptide was reported to specifically bind to the fribronectin-fibrin complexes in the extracellular matrix of different tumors with little binding to normal tissues.17 It is plausible to speculate that increased tumor enhancement with the CLT_1-targeted nanoglobular-[Mn(II)-DOTA] conjugate resulted from the specific binding of the CLT1 peptide to the cancer-related fibronectin in tumor tissue. Although the non-targeted Mn(II)-based nanoglobular agent could passively accumulate in tumor due to tumor vascular hyperpermeability, tumor enhancement of the non-targeted agent was much less than the corresponding nanoglobular Mn-DOTA conjugate. In contrast, the targeted agent delivered a sufficient amount of the Mn(II) chelates due to target-specific binding in tumor stroma, resulting in significant tumor enhancement.

The nanoglobules have a compact spheric morphology with a highly functionalized surface that can accommodate targeting agents and a relatively large number of paramagnetic chelates. The G3 nanoglobule has 64 amino groups available for chemical conjugation, while a conventional G3 PAMAM dendrimer has only 16 surface amino groups available for conjugation.27, 28 The unique structural of the nanoglobule allows the conjugation of targeted agents and a relatively large amount of chelates without substantial increase of the size of the contrast agent. As a result, the targeted nanoglobular Mn(II)-DOTA monoamide conjugate had high overall relaxivities. The globular structure of the targeted contrast agent also minimizes the steric effect of the carrier for specific binding of the agent to the biomarker. Since oncofetal fibronectin is highly expressed in the stroma of malignant tumors, the targeted nanoglobular agent of a relatively small nanosize could readily diffuse into the tumor tissue and effectively bind to the molecular target. The targeted nanoglobular contrast agent is able to deliver sufficient Mn(II) chelates to tumor tissue to overcome the limitation of low relaxivity and to generate detectable signal enhancement for MR molecular imaging.

The nanoglobular Mn(II)-DOTA monoamide conjugates demonstrated good in vivo stability as evidenced by low contrast enhancement in the liver and myocardium with both the targeted contrast agent and control agent. It has been reported that free Mn(II) ions have high accumulation in the liver and myocardium, resulting in strong contrast enhancement in these organs.8, 29 Mn(II) chelates with low stability would dissociate in vivo by transmetallation with free Ca^{2+} and Mg^{2+} ions in plasma to release free Mn(II) ions from Mn-based contrast agents. The dynamic 3D MR images of targeted and non-targeted nanoglobular contrast agents showed strong bladder enhancement and only slight enhancement in the liver and myocardium during the period of experiment, indicating high in vivo stability of the Mn(II) based contrast agents and their excretion as intact chelates. It might be attributed to high thermodynamic and kinetic stability of macrocyclic DOTA chelates towards transmetallation.

To our best knowledge, this is the first study of successfully using targeted Mn(II)-chelates for effective cancer MR molecular imaging. The targeted nanoglobular Mn-DOTA monoamide conjugate is advantageous over the corresponding nanoglobular Gd(III) based contrast agent in term of better safety profile. Manganese is an essential element in the body and much less toxic than gadolinium. This study demonstrated that the targeted nanoglobular Mn-DOTA conjugate could provide sufficient contrast enhancement in the target tissue at a low dose. The agent was readily excreted via renal filtration with minimal non-specific liver accumulation. Mn(II) The CLT1 peptide targeted nanoglobular Mn(II)-DOTA monoamide conjugate is a promising non-Gd(III) based MRI contrast agent for effective cancer MR molecular imaging. Further studies are needed to optimize the structure

of the Mn(II) based targeted contrast agents and to demonstrate their safety for further development.

Conclusions

We designed and synthesized a CLT1 peptide-targeted nanoglobular Mn(II)-DOTA monoamide conjugate for cancer MR molecular imaging. The targeted nanoglobular contrast agent had a well-defined size and could be readily excreted via renal filtration. The Mn(II) chelates had a good in vivo stability and resulted in little non-specific enhancement in the liver and myocardium. The CLT1-targeted contrast agent resulted in significant contrast enhancement in tumor at a relatively low dose as compared to the non-targeted control. The CLT1-targeted nanoglobular Mn-DOTA conjugate has a potential to be further developed as a non-Gd(III) based MRI contrast agent for MR cancer molecular imaging.

Supplementary Material

Refer to Web version on PubMed Central for supplementary material.

Acknowledgments

This work is supported in part by the NIH R01 CA097465. We greatly appreciate Dr. Yongen Sun and Mr. Xianfeng Shi, for technical assistance in animal handing and MRI data acquisition.

References

1. Kozlowska D, Foran P, MacMahon P, Shelly M, Eustace S, O'Kennedy R. Molecular and magnetic resonance imaging: The value of immunoliposomes. Adv. Drug Deliver. Rev. 2009; 61(15):1402–1411.
2. Aime S, Castelli D, Crich S, Gianolio E, Terreno E. Pushing the sensitivity envelope of lanthanide-based magnetic resonance imaging (MRI) contrast agents for molecular imaging applications. Accounts. Chem. Res. 2009; 42(7):822–831.
3. Briley-Saebo K, Mulder W, Mani V, Hyafil F, Amirbekian V, Aguinaldo J, Fisher E, Fayad Z. Magnetic resonance imaging of vulnerable atherosclerotic plaques: Current imaging strategies and molecular imaging probes. J Magn Reson Imaging. 2007; 26(3):460–479. [PubMed: 17729343]
4. Ye F, Ke T, Jeong E, Wang X, Sung Y, Johnson M, Lu Z. Noninvasive visualization of in vivo drug delivery of poly(L-glutamic acid) using contrast-enhanced MRI. Mol. Pharm. 2006; 3(5):507–515. [PubMed: 17009849]
5. Mohs A, Lu Z. Gadolinium(III)-based blood-pool contrast agents for magnetic resonance imaging: status and clinical potential. Expert Opin Drug Deliv. 2007; 4(2):149–164. [PubMed: 17335412]
6. Marckmann P, Skov L, Rossen K, Dupont A, Damholt M, Heaf J, Thomsen H. Nephrogenic systemic fibrosis: Suspected causative role of gadodiamide used for contrast-enhanced magnetic resonance imaging. J. Am. Soc. Nephrol. 2006; 17(9):2359–2362. [PubMed: 16885403]
7. Yu X, Wadghiri Y, Sanes D, Turnbull D. In vivo auditory brain mapping in mice with Mn-enhanced MRI. Nat. Neurosci. 2005; 8(7):961–968. [PubMed: 15924136]
8. Waghorn B, Yang Y, Baba A, Matsuda T, Schumacher A, Yanasak N, Hu T. Assessing manganese efflux using SEA0400 and cardiac T-1-mapping manganese-enhanced MRI in a murine model. NMR Biomed. 2009; 22(8):874–881. [PubMed: 19593760]
9. Crossgrove J, Zheng W. Manganese toxicity upon overexposure. NMR Biomed. 2004; 17(8):544–553. [PubMed: 15617053]
10. Bertin A, Steibel J, Michou-Gallani A, Gallani J, Felder-Flesch D. Development of a dendritic manganese-enhanced magnetic resonance imaging (MEMRI) contrast agent: synthesis, toxicity (in vitro) and relaxivity (in vitro, in vivo) studies. Bioconjugate Chem. 2009; 20:760–767.
11. Helms B, Meijer E. Dendrimers at work. Science. 2006; 313:929–930. [PubMed: 16917051]

12. Langereis S, de Lussanet Q, van Genderen M, Backes W, Meijer E. Multivalent contrast agents based on gadolinium-diethylenetriaminepentaacetic acid-terminated poly(propyleneimine) dendrimers for magnetic resonance imaging. Macromolecules. 2004; 37:3084–3091.
13. Kaneshiro T, Wang X, Lu Z. Synthesis, characterization, and gene delivery of Poly-L-lySine octa(3-aminopropyl)silsesquioxane dendrimers: nanoglobular drug carriers with precisely defined molecular Architectures. Mol. Pharmaceutics. 2007; 4(5):759–768.
14. Kaneshiro T, Jeong E, Morrell G, Parker D, Lu Z. Synthesis and evaluation of globular Gd-DOTA-monoamide conjugates with precisely controlled nanosizes for magnetic resonance angiography. Biomacromolecules. 2008; 9:2742–2748. [PubMed: 18771313]
15. Tan M, Wu X, Jeong E, Chen Q, Lu Z. Peptide-Targeted Nanoglobular Gd-DOTA Monoamide Conjugates for Magnetic Resonance Cancer Molecular Imaging. Biomacromolecules. 2010; 11(3): 754–761. [PubMed: 20131758]
16. Ye F, Jeong E, Jia Z, Yang T, Parker D, Lu Z. A peptide targeted contrast agent specific to fibrin-fibronectin complexes for cancer molecular imaging with MRI. Bioconjugate Chem. 2008; 19(12): 2300–2303.
17. Pilch J, Brown DM, Komatsu M, Jarvinen TAH, Yang M, Peters D, Hoffman RM, Ruoslahti E. Peptides selected for binding to clotted plasma accumulate in tumor stroma and wounds. Proc. Natl. Acad. Sci. USA. 2006; 103:2800–2804. [PubMed: 16476999]
18. Loridonrosa B, Vielh P, Matsuura H, Clausen H, Cuadrado C, Burtin P. Distribution of oncofetal fibronectin in human mammary-tumors - immunofluorescence study on histological sections. Cancer Res. 1990; 50(5):1608–1612. [PubMed: 2406016]
19. Kaspar M, Zardi L, Neri D. Fibronectin as target for tumor therapy. Int. J Cancer. 2006; 118(6): 1331–1339. [PubMed: 16381025]
20. Yang C, Li Y, Liu S. Synthesis and structural characterization of complexes of a DO3A-conjugated triphenylphosphonium cation with diagnostically important metal ions. Inorg Chem. 2007; 46(21):8988–8997. [PubMed: 17784751]
21. Kolb H, Finn M, Sharpless K. Click chemistry: Diverse chemical function from a few good reactions. Angew. Chem. Int. Edit. 2001; 40(11):2004–2021.
22. Byegard J, Skarnemark G, Skalberg M. The stability of some metal EDTA, DTPA and DOTA complexes: Application as tracers in groundwater studies. J. Radioanal. Nucl. Ch. 1999; 241(2): 281–290.
23. Balogh E, Tripier R, Fouskova P, Reviriego F, Handel H, Toth E. Monopropionate analogues of DOTA(4-) and DTPA(5-): kinetics of formation and dissociation of their lanthanide(III) complexes. Dalton T. 2007; (32):3572–3581.
24. Wu X, Zong Y, Ye Z, Lu Z-R. Stability and biodistribution of a biodegradable macromolecular MRI contrast agent Gd-DTPA cystamine copolymers (GDCC) in rats. Pharm. Res. 2010 in press. (DOI: 10.1007/s11095-010-0131-9).
25. Longmire M, Choyke P, Kobayashi H. Clearance properties of nano-sized particles and molecules as imaging agents: considerations and caveats. Nanomedicine. 2008; 3(5):703–717. [PubMed: 18817471]
26. Lauffer R. Paramagnetic metal-complexes as water proton relaxation agents for nmr imaging - theory and design. Chem. Rev. 1987; 87(5):901–927.
27. Boswell C, Eck P, Regino C, Bernardo M, Wong K, Milenic D, Choyke P, Brechbiel M. Synthesis, characterization, and biological evaluation of integrin alpha(v)beta(3)-targeted PAMAM dendrimers. Mol. Pharmaceutics. 2008; 5(4):527–539.
28. Ali M, Yoo B, Pagel M. Tracking the Relative In Vivo Pharmacokinetics of Nanoparticles with PARACEST MRI. Mol. Pharmaceutics. 2009; 6(5):1409–1416.
29. Wisner E, Merisko-liversidge E, Kellar K, Katzberg R, Karpinski P, Amparo E, Drake C, Griffey S, Brock J. Preclinical evaluation of manganese carbonate particles for magnetic-resonance-imaging of the liver. Acad Radiol. 1995; 2(2):140–147. [PubMed: 9419538]

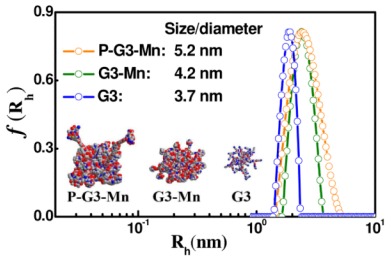

Figure 1.

Hydrodynamic radius (R_h) distributions $f(R_h)$ of peptide CLT1-targeted G3-DOTA-Mn (P-G3-Mn), G3-DOTA-Mn (G3-Mn) conjugates and G3 nanoglobule in deionized water at 25 °C.

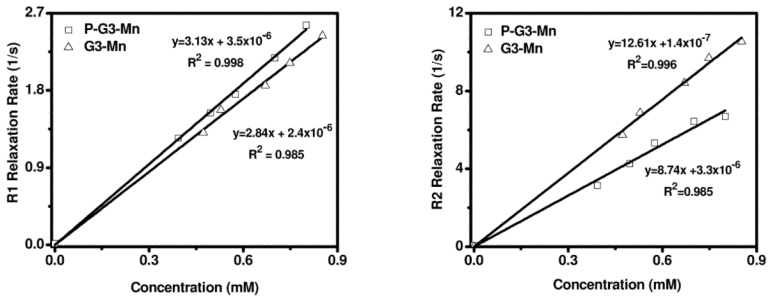

Figure 2.

Longitudinal relaxivity rate (left) and transverse relaxivity rate (right) of peptide CLT1-targeted G3-DOTA-Mn (P-G3-Mn) and the control nanoglobular conjugate G3-DOTA-Mn (G3-Mn) as a function of Mn(II) concentration.

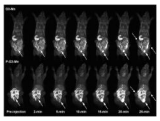

Figure 3.
Representative 3D maximum intensity projection images (T_1-weighted) of a tumor bearing mouse injected with G3-DOTA-Mn (G3-Mn) and peptide CLT1-targeted G3-DOTA-Mn (P-G3-Mn) nanoglobular MRI contrast agent at 30 μmol-Mn/kg. Solid arrows show urinary bladder and dashed arrows show tumor.

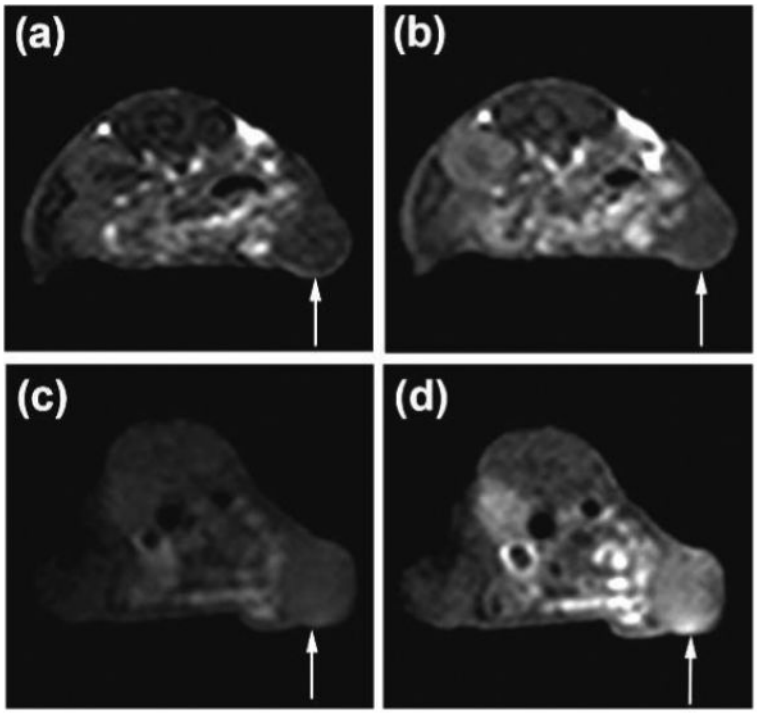

Figure 4.
2D axial MR images (T_1-weighted) of tumor xenografts before (a) and 25 min after (b) the administration of G3-DOTA-Mn, and before (c) and 25 min after (d) the administration of peptide CLT1-targeted G3-Mn. Arrows point tumors.

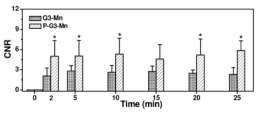

Figure 5.
CNR in the tumor with peptide CLT1-targeted G3-DOTA-Mn (P-G3-Mn) and G3-DOTA-Mn (G3-Mn) administrated at 0.03 mmol-Mn/kg in the tumor bearing mice. *$p < 0.05$.

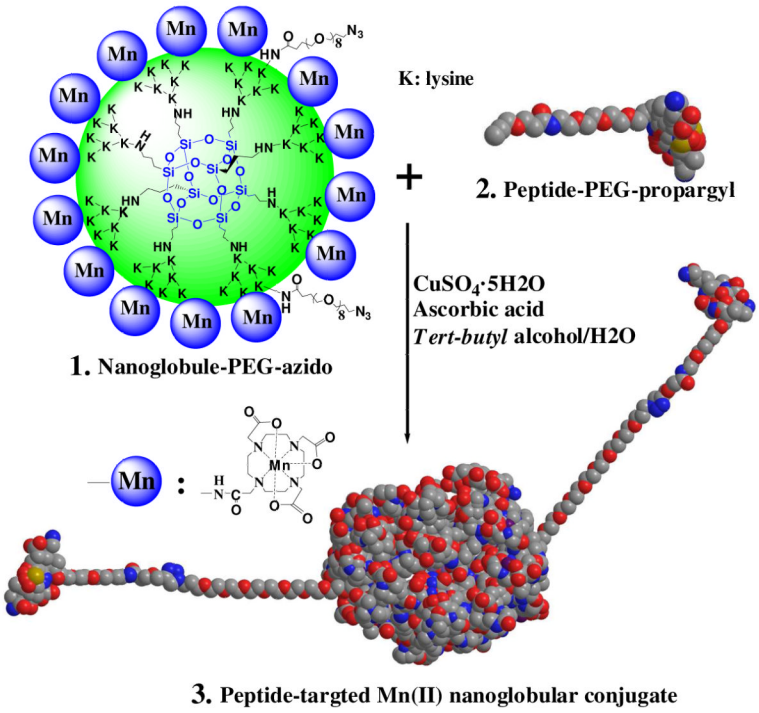

Scheme 1.
Synthetic scheme of a peptide CLT1-targeted nanoglobular Mn(II)-DOTA conjugate via click chemistry.

Table 1

Physicochemical properties of the nanoglobular MRI contrast agents

Contrast agents	Mn content mmol Mn/g dendrimer	Particle size (nm)	No. of surface Peptide	r_1/r_2 [mM^{-1}(Mn)s^{-1}] at 3T	r_1/r_2 [mM^{-1}(nanoglobule) s^{-1}] at 3T
P-G3-Mn	1.31	~ 5.2	~ 2	3.13/8.74	131.46/367.08
G3-Mn	1.46	~ 4.2	0	2.84/12.61	127.80/567.45

P-G3-Mn: peptide CLT1-targeted G3-DOTA-Mn; G3-Mn: G3-DOTA-Mn